

A nonintrusive method to approximate linear systems with nonlinear parameter dependence

June 7, 2021

Fabien Casenave¹, Alexandre Ern¹, Tony Lelièvre^{1,2}, and Guillaume Sylvand³

¹ Université Paris-Est, CERMICS (ENPC), 6-8 Avenue Blaise Pascal, Cité Descartes ,
F-77455 Marne-la-Vallée, France

² INRIA Rocquencourt, MICMAC Team-Project, Domaine de Voluceau, B.P. 105, 78153 Le
Chesnay Cedex, France

³ EADS-IW, 18 rue Marius Terce, 31300 Toulouse, France

Abstract

We consider a family of linear systems $A_\mu \alpha = C$ with system matrix A_μ depending on a parameter μ and for simplicity parameter-independent right-hand side C . These linear systems typically result from the finite-dimensional approximation of a parameter-dependent boundary-value problem. We derive a procedure based on the Empirical Interpolation Method to obtain a separated representation of the system matrix in the form $A_\mu \approx \sum_m \beta_m(\mu) A_{\mu_m}$ for some selected values of the parameter. Such a separated representation is in particular useful in the Reduced Basis Method. The procedure is called nonintrusive since it only requires to access the matrices A_{μ_m} . As such, it offers a crucial advantage over existing approaches that instead derive separated representations requiring to enter the code at the level of assembly. Numerical examples illustrate the performance of our new procedure on a simple one-dimensional boundary-value problem and on three-dimensional acoustic scattering problems solved by a boundary element method.

1 Introduction

In industrial projects, decisions are often taken after a series of complex computations using computer codes of various origins. To simplify the overall computation, surrogate models can be used to replace some parts of the computation. Some of these surrogates are constructed using only a series of input/output couples. With some hypotheses on the input, confidence intervals can be derived, see e.g. [9] for the kriging method. When additional knowledge on the underlying mathematical formulation is available, model reduction methods can be used. For instance, the Reduced Basis Method (RBM) enables fast resolutions on a basis of precomputed solutions, rather than on a finite element basis (see [8] for a detailed presentation and [2] for some convergence results). We consider a family of linear systems $A_\mu \alpha = C$ of

order n , where n is large. For simplicity, we assume that the right-hand side is independent of the parameter μ .

The RBM consists first in an offline stage, where a reduced basis of \hat{n} functions u_j , $1 \leq j \leq \hat{n}$ are computed using a greedy algorithm. These functions are solution of the original problem for some values $(\mu_j)_{1 \leq j \leq \hat{n}}$ of the parameter μ , which are selected using a greedy algorithm. The functions u_j thus write $u_j(x) = \sum_{i=1}^n \alpha_i(\mu_j) \theta_i(x)$, where $(\theta_i)_{1 \leq i \leq n}$ is the finite element basis and the vector $\alpha(\mu_j) = (\alpha_i(\mu_j))_{1 \leq i \leq n}$ is such that $A_{\mu_j} \alpha(\mu_j) = C$. In practice, the dimension of the reduced basis is much smaller than the dimension of the finite element basis: $\hat{n} \ll n$. Denote by U the rectangular matrix of size $n \times \hat{n}$ such that $(U)_{i,j} = \alpha_i(\mu_j)$. Second, in the online stage, for a given value of the parameter μ , a reduced problem is constructed as $\hat{A}_\mu \hat{\alpha}(\mu) = \hat{C}$, where $\hat{A}_\mu = U^t A_\mu U$ and $\hat{C} = U^t C$. Solving this reduced problem for a certain value of μ leads to the approximate solution $\hat{u}_\mu(x) = \sum_{j=1}^{\hat{n}} \hat{\alpha}_j(\mu) u_j(x)$.

To efficiently construct the online problems, a separated representation (also known as an *affine decomposition* in the RBM literature) of the matrix assembled by the code is needed in the form

$$A_\mu \approx \sum_{m=1}^d \gamma_m(\mu) A_m, \quad (1)$$

so that

$$\hat{A}_\mu \approx \sum_{m=1}^d \gamma_m(\mu) U^t A_m U, \quad (2)$$

where the matrices $U^t A_m U$ are of small size $\hat{n} \times \hat{n}$ and can be precomputed during the offline stage. The separated representation (1) thus enables online problems to be constructed in complexity independent of n , as long as the functions $\mu \mapsto \gamma_m(\mu)$ are also computed in complexity independent of n . Standard techniques (see [6]) to obtain the separated representation (1) require in general nontrivial modifications of the assembling routines of the computational code in order to access separately various terms of the variational formulation at hand (See Remark 3.3 below for more details).

The present work provides a step forward in this context, since a procedure that yields a separated representation of A_μ in the form

$$A_\mu \approx \sum_{m=1}^d \beta_m(\mu) A_{\mu_m} \quad (3)$$

is derived, where $(\mu_m)_{1 \leq m \leq d}$ are some selected values of the parameter. Since the separated representation (3) only uses the complete system matrix at the selected parameter values, this representation requires no implementation effort in the assembly routines of the computational code under the (mild) assumptions that we can indeed access the system matrix A_μ and that we can identify the functional dependencies on μ in the variational formulation under consideration (see below for more details). For this reason, the procedure is called nonintrusive.

In Section 2, we present the approximation problems investigated in this work, first a simple introductory example and then problems with a more complex parameter dependence. In Section 3, we briefly recall the Empirical Interpolation Method. In Section 4, we present our nonintrusive procedure for the introductory example and test it on a one-dimensional boundary-value problem. The procedure is extended to more complex parameter dependence in Section 5 where it is also applied to two three-dimensional scattering problems. Some conclusions are drawn in Section 6 where, in particular, we observe that our procedure can be extended to the approximation of other quantities.

2 The approximation problem

We first present an introductory example. Let \mathcal{V} be a Hilbert space and consider the following weak formulation: Find $u \in \mathcal{V}$ such that for all $u^t \in \mathcal{V}$,

$$\int_{\Omega} g(\mu, x) \nabla u(x) \cdot \nabla u^t(x) dx + \int_{\Omega} \mu u(x) u^t(x) dx = b(u^t), \quad (4)$$

where Ω is the domain of computation, μ a parameter belonging to a given parameter set \mathcal{P} , $g(\mu, x)$ a given function defined on $\mathcal{P} \times \Omega$ and b a bounded linear form on \mathcal{V} . Consider now a conforming n -dimensional approximation of the space \mathcal{V} denoted by \mathcal{V}_h (the subscript h refers to an underlying mesh), and a basis of \mathcal{V}_h denoted by $(\theta_i)_{1 \leq i \leq n}$. The finite element approximation of (4) requires the computation of the matrix A_μ of size $n \times n$ with entries

$$(A_\mu)_{i,j} := \left(\int_{\Omega} g(\mu, x) \nabla \theta_j(x) \cdot \nabla \theta_i(x) dx + \mu \int_{\Omega} \theta_j(x) \theta_i(x) dx \right)_{i,j}. \quad (5)$$

The notation A_μ is adopted to stress the fact that the matrix A_μ depends on the value of the parameter μ . The problem solved by the computational code is

$$A_\mu \alpha = C, \quad (6)$$

where $(C)_i = b(\theta_i)$ for all $1 \leq i \leq n$, and where an approximation of the solution u to (4) is obtained in the form $u(x) \approx \sum_{i=1}^n \alpha_i \theta_i(x)$.

Let

$$(A_\mu^1)_{i,j} := \left(\int_{\Omega} g(\mu, x) \nabla \theta_j(x) \cdot \nabla \theta_i(x) dx \right)_{i,j} \quad \text{and} \quad (A^0)_{i,j} := \left(\int_{\Omega} \theta_j(x) \theta_i(x) dx \right)_{i,j} \quad (7)$$

so that

$$A_\mu = A_\mu^1 + \mu A^0. \quad (8)$$

Definition 2.1 (Intrusivity). *A procedure leading to a separated representation of A_μ in the general form (1) is called*

- *intrusive if it requires to implement new integral terms,*
- *weakly-intrusive if it only requires to precompute independently A_μ^1 for some values of μ and A^0 ,*
- *nonintrusive if it only requires to precompute A_μ for some values of μ .*

The term “weakly-intrusive” comes from the fact that the user has to enter the routines of the code and to insert switches at the right places to save the terms in A_μ^1 independently from the terms in A^0 . In the context of industrial codes, this is not always possible. The notion of nonintrusivity in Definition 2.1 is different from the notion of black-box, which requires only the computation of input / output couples. Our purpose is to develop a nonintrusive procedure leading to the separated representation (3) of A_μ .

The above example can be generalized to a class of engineering problems requiring to compute a large, parameter-dependent matrix A_μ for many values of the parameter μ where A_μ is of the form

$$A_\mu = \sum_{\varrho=1}^R A_\mu^\varrho + \sum_{s=1}^S \psi_s(\mu) A^s, \quad (9)$$

where A_μ^g are matrices that require to integrate some functions $g^g(\mu, x)$ over Ω , ψ^s are given functions of μ and A^s are μ -independent matrices resulting from some integration over Ω . The introductory example corresponds to $R = 1$, $S = 1$, and $\psi_1(\mu) = \mu$. To simplify the presentation of the main ideas, we consider the setting of (8) in Sections 3 and 4 and return to the more general setting of (9) in Section 5.

3 Empirical Interpolation Method

The Empirical Interpolation Method (EIM) is a procedure to approximate two-variable functions. In particular, it can be used to approximate the two-variable function $g(\mu, x)$, for all $\mu \in \mathcal{P}$ and all $x \in \Omega$. Denote by EIM^g this particular procedure. EIM^g leads to an interpolation operator $I_{d^g}^g$ such that

$$(I_{d^g}^g g)(\mu, x) \approx g(\mu, x), \quad \forall \mu \in \mathcal{P}, \forall x \in \Omega, \quad (10)$$

where d^g is the number of interpolation points (called *magic points* in the context of BRM, see [6]). EIM^g is composed of two stages: (i) an offline stage, where a matrix B^g of size $d^g \times d^g$, a set of d^g x -dependent basis functions $\{q_k^g\}_{1 \leq k \leq d^g}$, a set of d^g points $\{x_k\}_{1 \leq k \leq d^g}$ in Ω , and a set of d^g parameter values $\{\mu_k\}_{1 \leq k \leq d^g}$ in \mathcal{P} are constructed, (ii) an online stage, where the quantities computed in the offline stage are used to carry out the approximation (10) (see Section 4.2 for more details on the offline / online stages for the whole procedure).

The offline stage of EIM^g is detailed in Algorithm 1. In the loop on k in Algorithm 1, the residual operator δ_k^g is defined by $\delta_k^g = \text{Id} - I_k^g$, where the interpolation operator I_k^g is such that

$$(I_k^g g)(\mu, x) := \sum_{m=1}^k \lambda_m^g(\mu) q_m^g(x), \quad (11)$$

and for a given $\mu \in \mathcal{P}$, the $\lambda_m^g(\mu)$'s are defined by

$$\sum_{m=1}^k B_{l,m}^g \lambda_m^g(\mu) = g(\mu, x_l^g), \quad \forall 1 \leq l \leq k. \quad (12)$$

After d^g iterations, the interpolation formula (11) leads to the following approximation for A_μ :

$$A_\mu \approx \sum_{m=1}^{d^g} \lambda_m^g(\mu) M_m + \mu A^0, \quad (13)$$

where $(M_m)_{i,j} = \int_{\Omega} q_m^g(x) \vec{\nabla} \theta_j(x) \cdot \vec{\nabla} \theta_i(x) dx$. This representation of A_μ is of the form (1).

Property 3.1 (Interpolation). $\forall x \in \Omega, \forall 1 \leq m \leq d^g, (I_{d^g}^g g)(\mu_m^g, x) = g(\mu_m^g, x)$.

Proof. See [6, Lemma 1]. □

Property 3.1 means that, at the parameter values $(\mu_k^g)_{1 \leq k \leq d^g}$ selected by EIM^g , the approximation (13) is exact since $\sum_{m=1}^{d^g} \lambda_m^g(\mu_k^g) M_m = A_{\mu_k^g}^1$ for all $1 \leq k \leq d^g$. Since $\text{Vect}_{1 \leq k \leq d^g}(q_k^g(x)) = \text{Vect}_{1 \leq k \leq d^g}(g(\mu_k^g, x))$ holds in Algorithm 1, the functions $q_k^g(x)$ can be expressed in terms of the functions $g(\mu_k^g, x)$ in the following form: there exist $\gamma_{l,k}, 1 \leq l \leq$

Algorithm 1 Offline stage of EIM^g

1. Choose $d^g > 1$ [Number of interpolation points]
 2. Set $k := 1$
 3. Compute $\mu_1^g := \operatorname{argmax}_{\mu \in \mathcal{P}} \|g(\mu, \cdot)\|_{L^\infty(\Omega)}$
 4. Compute $x_1^g := \operatorname{argmax}_{x \in \Omega} |g(\mu_1^g, x)|$ [First interpolation point]
 5. Set $q_1^g(\cdot) := \frac{g(\mu_1^g, \cdot)}{g(\mu_1^g, x_1^g)}$ [First basis function]
 6. Set $B_{1,1}^g := 1$ [Initialize B^g matrix]
 7. **while** $k \leq d^g$ **do**
 8. Compute $\mu_{k+1}^g := \operatorname{argmax}_{\mu \in \mathcal{P}} \|(\delta_k^g g)(\mu, \cdot)\|_{L^\infty(\Omega)}$
 9. Compute $x_{k+1}^g := \operatorname{argmax}_{x \in \Omega} |(\delta_k^g g)(\mu_{k+1}^g, x)|$ [($k+1$)-th interpolation point]
 10. Set $q_{k+1}^g(\cdot) := \frac{(\delta_k^g g)(\mu_{k+1}^g, \cdot)}{(\delta_k^g g)(\mu_{k+1}^g, x_{k+1}^g)}$ [($k+1$)-th basis function]
 11. Set $B_{i,k+1}^g := q_{k+1}^g(x_i^g)$, for all $1 \leq i \leq k+1$ [Increment matrix B^g]
 12. $k \leftarrow k+1$ [Increment the size of the interpolation]
 13. **end while**
-

$k \leq d^g$ such that $q_k^g(x) = \sum_{l=1}^{d^g} \gamma_{l,k} g(\mu_l^g, x)$, for all $1 \leq k \leq d^g$. Letting $(\lambda_m^g(\mu))_{1 \leq m \leq d^g}$ solve (12) for $k = d^g$, we obtain after exchanging the summations

$$(I_{d^g}^g g)(\mu, x) = \sum_{m=1}^{d^g} \left(\sum_{l=1}^{d^g} \gamma_{m,l} \lambda_l^g(\mu) \right) g(\mu_m^g, x). \quad (14)$$

Define $\eta_m^g(\mu) := \sum_{l=1}^{d^g} \gamma_{m,l} \lambda_l^g(\mu)$. The following property then holds:

Property 3.2 (Weak-intrusivity). EIM^g leads to a weakly-intrusive procedure, since the resulting approximation of A_μ can be written

$$A_\mu \approx \sum_{m=1}^{d^g} \eta_m^g(\mu) A_{\mu_m^g}^1 + \mu A^0. \quad (15)$$

Remark 3.3 (Comparison with the standard EIM procedure in the RBM literature). *If the considered variational formulation contains only one term, the above procedure was already proposed in the RBM literature as a nonintrusive method to obtain a separated representation of the linear system under consideration, see [6]. For instance in (15), if $A^0 = 0$, then $A_{\mu_m^g}^1 = A_{\mu_m^g}$. In the general setting of (9), this corresponds to $R = 1$ and $S = 0$. In any other case, the classical EIM needs to access independently matrices associated to each term of the variational formulation and thus cannot deliver a separated representation solely based on the A_μ matrices.*

4 The nonintrusive procedure

4.1 Description of the procedure

Denote by $G^g(\mu)$ the vector-valued function with d^g components such that $G_m^g(\mu) = g(\mu, x_m^g)$, for all $1 \leq m \leq d^g$. Then, from (12), $\lambda^g(\mu) = (\lambda_m^g(\mu))_{1 \leq m \leq d^g}$ can be concisely written as $\lambda^g(\mu) = (B^g)^{-1} G^g(\mu)$. Notice that the computation of $\lambda^g(\mu)$ only requires the matrix B^g and the set of points $\{x_m^g\}_{1 \leq m \leq d^g}$. Let $(z_p(\mu))_{1 \leq p \leq d_{\max}}$ with $d_{\max} := d^g + 1$, be such that

$$z_p(\mu) := \begin{cases} \lambda_p^g(\mu) & 1 \leq p \leq d^g, \\ \mu & p = d^g + 1. \end{cases} \quad (16)$$

Recalling the notation $(M_m)_{i,j} := \int_{\Omega} q_m^g(x) \vec{\nabla} \theta_j(x) \cdot \vec{\nabla} \theta_i(x) dx$ for all $1 \leq m \leq d^g$, we infer from (13) that

$$A_\mu \approx \sum_{m=1}^{d^g} \lambda_m^g(\mu) M_m + \mu A^0 = \sum_{p=1}^{d_{\max}} z_p(\mu) T_p, \quad (17)$$

where the matrices

$$T_p := \begin{cases} M_p & 1 \leq p \leq d^g, \\ A^0 & p = d^g + 1 = d_{\max}, \end{cases} \quad (18)$$

are independent of μ . Note that d_{\max} is the number of matrices to precompute and store when using the approximation (13).

The key idea is now to apply a second EIM to approximate $z_p(\mu)$, where z is seen as a function depending on the two variables p and μ . The EIM procedure to approximate $z_p(\mu)$ is denoted by EIM^z and its offline stage is detailed in Algorithm 2. The number of interpolation points is denoted by $d^z \leq d_{\max}$. In the loop on k in Algorithm 2, the residual operator δ_k^z is defined by $\delta_k^z = \text{Id} - I_k^z$, where

$$(I_k^z z)_p(\mu) := \sum_{m=1}^k \beta_m^z(\mu) z_p(\mu_m^z), \quad (19)$$

and

$$\sum_{m=1}^k B_{m,l}^z \beta_m^z(\mu) = q_l^z(\mu), \quad 1 \leq l \leq k. \quad (20)$$

Owing to the interpolation property, there holds $(I_{d^z}^z z)_{p_k^z}(\mu) = z_{p_k^z}(\mu)$ for all $1 \leq k \leq d^z$ and all $\mu \in \mathcal{P}$. If $d^z = d_{\max}$, all the indices p are selected in Algorithm 2 and $(I_{d_{\max}}^z z)_p(\mu) = z_p(\mu)$ for all $1 \leq p \leq d_{\max}$ and all $\mu \in \mathcal{P}$. Observe that we can stop EIM^z before $d^z = d_{\max}$ interpolation matrices have been computed, see Sections 5.2 and 5.3 for some illustrations.

Injecting the approximation (19) with $k = d^z$ into the right-hand side of (17) with $z_p(\mu)$ replaced by $(I_{d^z}^z z)_p(\mu)$ yields

$$A_\mu \approx \sum_{p=1}^{d_{\max}} T_p \sum_{m=1}^{d^z} \beta_m^z(\mu) z_p(\mu_m^z) = \sum_{m=1}^{d^z} \beta_m^z(\mu) \sum_{p=1}^{d_{\max}} T_p z_p(\mu_m^z) \approx \sum_{m=1}^{d^z} \beta_m^z(\mu) A_{\mu_m^z}, \quad (21)$$

where $\beta_m^z(\mu)$ is obtained from (20). The right-hand side of (21) is the desired separated representation of A_μ that can be built in a nonintrusive way.

Algorithm 2 Offline stage of EIM^z

1. Choose $d^z > 1$ [Number of interpolation points]
 2. Set $k := 1$
 3. Compute $p_1^z := \operatorname{argmax}_{1 \leq p \leq d^g+1} \|(z)_p(\cdot)\|_{L^\infty(\mathcal{P})}$
 4. Compute $\mu_1^z := \operatorname{argmax}_{\mu \in \mathcal{P}} |(z)_{p_1^z}(\mu)|$ [First interpolation point]
 5. Set $q_1^z(\cdot) := \frac{(z)_{p_1^z}(\cdot)}{(z)_{p_1^z}(\mu_1^z)}$ [First basis function]
 6. Set $B_{1,1}^z := 1$ [Initialize B^z matrix]
 7. **while** $k \leq d^z$ **do**
 8. Compute $p_{k+1}^z := \operatorname{argmax}_{1 \leq p \leq d^g+1} \|(\delta_k^z z)_p(\cdot)\|_{L^\infty(\mathcal{P})}$,
 9. Compute $\mu_{k+1}^z := \operatorname{argmax}_{\mu \in \mathcal{P}} |(\delta_k^z z)_{p_{k+1}^z}(\mu)|$ [$(k+1)$ -th interpolation point]
 10. Set $q_{k+1}^z(\cdot) := \frac{(\delta_k^z z)_{p_{k+1}^z}(\cdot)}{(\delta_k^z z)_{p_{k+1}^z}(\mu_{k+1}^z)}$ [$(k+1)$ -th basis function]
 11. $B_{i,k+1}^z := q_{k+1}^z(\mu_i^z)$, for all $1 \leq i \leq k+1$ [Increment matrix B^z]
 12. $k \leftarrow k+1$ [Increment the size of the interpolation]
 13. **end while**
-

4.2 Practical implementation

To compute the L^∞ -norms and determine the argmax in Algorithms 1 and 2, it is convenient to consider finite subsets of \mathcal{P} and Ω , denoted respectively by $\mathcal{P}_{\text{trial}}$ and Ω_{trial} . This becomes necessary when, for instance, the function $g(\mu, x)$ is not known analytically, but only for some elements of \mathcal{P} and Ω . It seems natural to take for Ω_{trial} the set of Gauss points on which the quadrature formulae to compute the integrals in (4) are defined. However, this supposes to know and manipulate the set of the Gauss points associated with the mesh. Since the functions q^g defined in Algorithm 1 are only used to construct the matrix B^g and are not directly integrated with respect to x to carry out the interpolation (21), it is possible to write the procedure with any set Ω_{trial} sampling the geometry. Such an approach is considered in the numerical example of Section 5.3. More generally, the sets $\mathcal{P}_{\text{trial}}$ and Ω_{trial} should be fine enough to capture all the phenomena, but not too fine to limit the overall computational cost. The numerical examples of Section 5 indicate that high accuracy can be obtained with simple choices for $\mathcal{P}_{\text{trial}}$ and Ω_{trial} .

In addition to the two sets $\mathcal{P}_{\text{trial}}$ and Ω_{trial} , the number of interpolation points d^g and d^z for each EIM have to be chosen. The choice we made is to stop the two EIM's when respectively $(\delta_k^g g)(\mu_{k+1}^g, x_{k+1}^g)$ and $(\delta_k^z z)_{p_{k+1}^z}(\mu_{k+1}^z)$ have reached a prescribed threshold, typically set at the level of the machine precision.

Finally, we specify the offline and online stages of our procedure when used within the RBM. EIM^g and the offline stage of EIM^z are part of the offline stage of the RBM. During the online stage of the RBM, the reduced matrix is constructed as

$$\hat{A}_\mu \approx \sum_{m=1}^{d^z} \beta_m^z(\mu) U^t A_{\mu_m^z} U, \quad (22)$$

so that only the online stage of EIM^z (i.e., the resolution of (20)) is needed.

4.3 Illustration

As a first illustration, we consider the following boundary-value problem:

$$-\frac{d}{dx} \left(\exp(\mu x) \frac{du}{dx}(x) \right) + \mu u(x) = 1 \quad \text{in } \Omega := (-3, 3), \quad (23)$$

with the following Dirichlet boundary condition $u(-3) = u(3) = 0$. The weak form reads: Find $u \in H_0^1(\Omega)$ such that for all $u^t \in H_0^1(\Omega)$,

$$a_\mu(u, u^t) = \int_\Omega u^t(x) dx, \quad (24)$$

with

$$a_\mu(u, u^t) := \int_\Omega \exp(\mu x) \frac{du}{dx}(x) \frac{du^t}{dx}(x) dx + \int_\Omega \mu u(x) u^t(x) dx. \quad (25)$$

First-order continuous Lagrange finite elements are used, with a three-point quadrature formula in each mesh cell. The mesh is uniform with $h_x = 0.015$. Ω_{trial} is taken to be the set of Gauss points on the obtained mesh, and $\mathcal{P}_{\text{trial}} = \{1, 1 + h_\mu, 1 + 2h_\mu, \dots, 3\}$ with $h_\mu = 0.005$. To derive the separated approximation (21), EIM^g is first applied to $g(\mu, x) := \exp(\mu x)$. Then, the vector-valued function $z(\mu)$ is constructed using (16). The quality of the whole procedure is measured, for various values of d^g and $d^z = d^g + 1$ using two error criteria: (i) the relative Frobenius norm error on the matrix A_μ and (ii) the relative $L^2(\Omega)$ -norm error on the solution, see Figures 1 and 2.

We conclude from this first test case that the present method allows for a very good approximation of the matrix and the solution.

5 Extension to more general parameter dependence

The goal of this section is to show how to extend the nonintrusive procedure described in Section 4 to more complex parameter dependence. We illustrate the procedure on an industrial test case, namely a frequency-dependent three-dimensional aeroacoustic scattering problem.

5.1 Generalization of the nonintrusive procedure

Recall the general form of the matrix A_μ to approximate:

$$A_\mu = \sum_{\varrho=1}^R A_\mu^\varrho + \sum_{s=1}^S \psi_s(\mu) A^s, \quad (26)$$

where A_μ^ϱ are matrices that require to integrate some functions $g^\varrho(\mu, x)$ over Ω , ψ^s are given functions of μ and A^s are μ -independent matrices resulting from some integration over Ω . EIM^g is applied independently to each $g^\varrho(\mu, x)$, for all $1 \leq \varrho \leq R$, where the number of interpolation points, respectively $(d^g)^\varrho$, may differ from one EIM^g to the other. These procedures lead to the construction of the functions $(\lambda_m^g)^\varrho(\mu)$, for all $1 \leq \varrho \leq R$, all $1 \leq m \leq (d^g)^\varrho$, and all $\mu \in \mathcal{P}_{\text{trial}}$, using (12). Then, define the functions $(z_p(\mu))_{1 \leq p \leq d_{\text{max}}}$ with $d_{\text{max}} := \sum_{\varrho=1}^R (d^g)^\varrho + S$

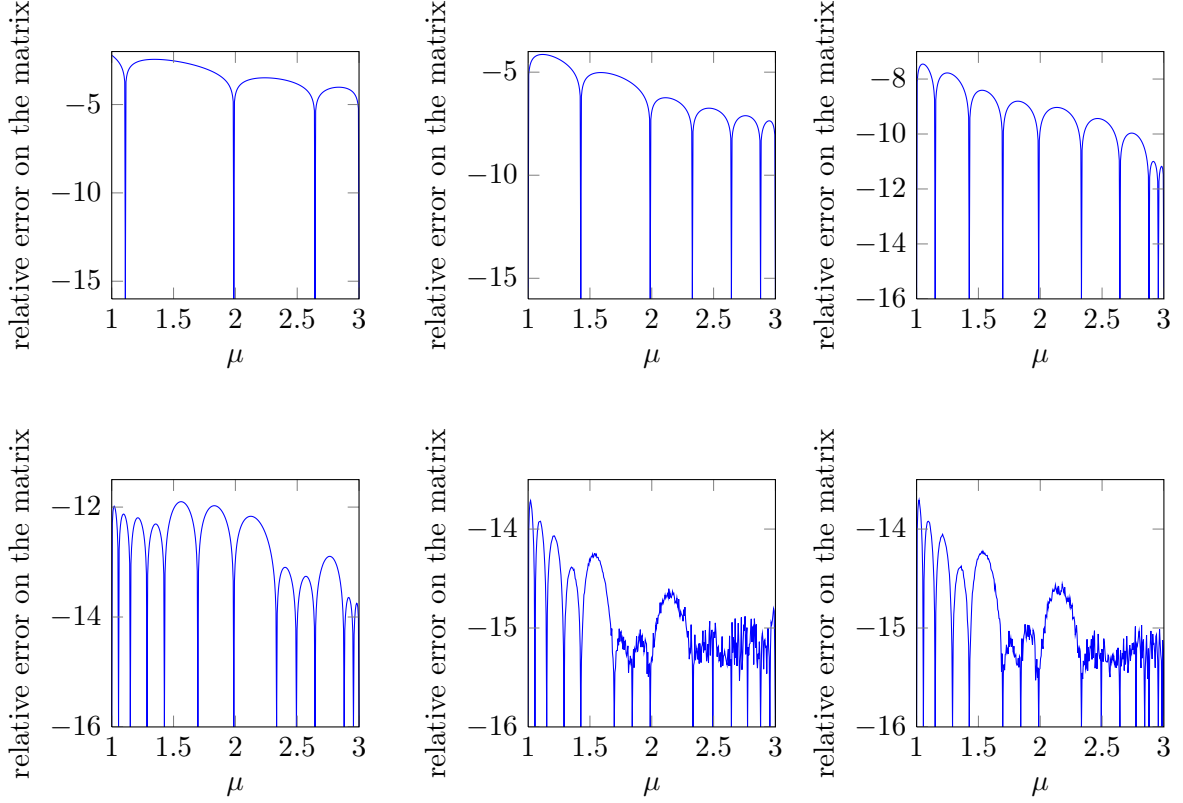


Figure 1: Log_{10} of the relative Frobenius norm error on the matrix A_μ for $d^g = 3, 6, 9, 12, 14, 16$, and $d^z = d^g + 1$.

such that

$$z_p(\mu) := \begin{cases} (\lambda_m^g)^1(\mu), & 1 \leq p \leq (d^g)^1, \quad m = p, \\ \vdots \\ (\lambda_m^g)^R(\mu), & 1 + \sum_{\varrho=1}^{R-1} (d^g)^\varrho \leq p \leq \sum_{\varrho=1}^R (d^g)^\varrho, \quad m = p - \sum_{\varrho=1}^{R-1} (d^g)^\varrho, \\ \psi_1(\mu), & p = \sum_{\varrho=1}^R (d^g)^\varrho + 1, \\ \vdots \\ \psi_S(\mu), & p = \sum_{\varrho=1}^R (d^g)^\varrho + S, \end{cases} \quad (27)$$

and let EIM^z be applied to $z_p(\mu)$, with d^z interpolation points, such that $d^z \leq d_{\max} = \sum_{\varrho=1}^R (d^g)^\varrho + S$, to obtain an approximation of A_μ in the same form as (21). Note that d_{\max} is the number of matrices to precompute and store when using the approximation (13), while the number of matrices to precompute and store when using (21) is d^z ; in our numerical examples (see below), accurate representations of A_μ are already achieved for d^z smaller than d_{\max} .

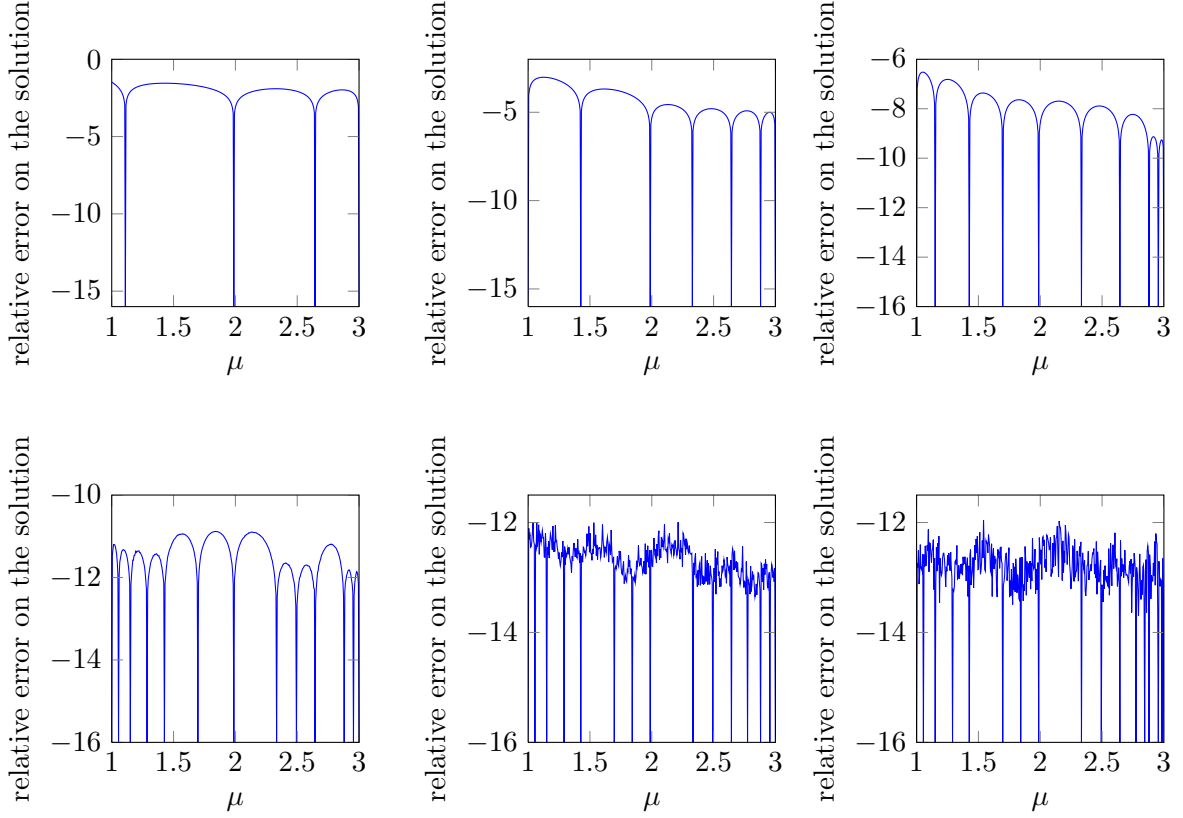


Figure 2: Log_{10} of the relative $L^2(\Omega)$ -norm error on the solution for $d^g = 3, 6, 9, 12, 14, 16$, and $d^z = d^g + 1$.

Notice also that in total, there are $(R + 1)$ EIM procedures to be applied.

5.2 Sound-hard scattering in the air at rest

The problem of interest is the sound-hard scattering of an acoustic monopole source of wave number μ by an aircraft (whose boundary is denoted by Γ) in the air at rest, in the time-harmonic case. To simulate the noise created by one of the engines, the monopole is located under the left wing of the plane. This is a classical Helmholtz exterior problem, for which one possible weak formulation is: Find $u \in H^{\frac{1}{2}}(\Gamma)$ such that for all $u^t \in H^{\frac{1}{2}}(\Gamma)$,

$$a_\mu(u, u^t) = \int_{\Gamma} f_{\text{inc}\mu}(x) u^t(x) dx, \quad (28)$$

where

$$a_\mu(u, u^t) := \frac{1}{4\pi} \int_{\Gamma} \int_{\Gamma} \frac{\exp(i\mu|x-y|)}{|x-y|} \left(\overrightarrow{\text{curl}}_{\Gamma} u(x) \cdot \overrightarrow{\text{curl}}_{\Gamma} u^t(y) \right) dx dy - \frac{\mu^2}{4\pi} \int_{\Gamma} \int_{\Gamma} \frac{\exp(i\mu|x-y|)}{|x-y|} u(x) u^t(y) (\overrightarrow{n}_x \cdot \overrightarrow{n}_y) dx dy, \quad (29)$$

where $\overrightarrow{\text{curl}}_{\Gamma}$ denotes the surfacic curl on Γ , \overrightarrow{n}_x the unit normal vector on Γ pointing towards the medium of propagation, and $f_{\text{inc}\mu}$ is the incident acoustic field created by the source.

	Mesh 1	Mesh 2
number of triangles	7,886	40,576
number of vertices	3,945	20,290
smallest edge (mm)	6.53	6.53
mean edge (mm)	437.52	192.92
largest edge (mm)	718.99	389.29
number of complex nonzero coefficients per matrix	1.56×10^7	4.12×10^8
memory usage to store one matrix in binary format (Go)	0.23	6.5

Table 1: Characteristics of the two considered meshes.

We refer to [7, Section 3.4] for details on the derivation of (28), and justifications on the well-posedness of the integral in (29). The parameter of interest is the wave number μ of the acoustic monopole source. The Boundary Element Method (BEM) is used to approximate problem (28). This leads to a dense μ -dependent matrix $(A_\mu)_{i,j} = a_\mu(\theta_j, \theta_i)$, where $(\theta_i)_{1 \leq i \leq n}$ denote the basis functions of the considered finite element space on Γ . Two different meshes, on which the matrices are assembled, are considered, see Table 1 and Figure 3. The in-house code ACTIPOLE developed by EADS-IW and Airbus [4, 5] is used. This test case is a challenging benchmark for two reasons. First, the Green kernel $G_\mu(x, y) := \frac{\exp(i\mu|x-y|)}{4\pi|x-y|}$ oscillates at a frequency proportional to the parameter of interest μ , and, secondly, the obtained matrices are dense and complex-valued. Mesh 2 leads to a very large matrix and cannot be stored in an average desktop computer RAM. The tests on Mesh 1 have been computed on a simple laptop with 4 Go of RAM, whereas the tests on Mesh 2 have been computed on CCRT's Curie supercomputer [1].

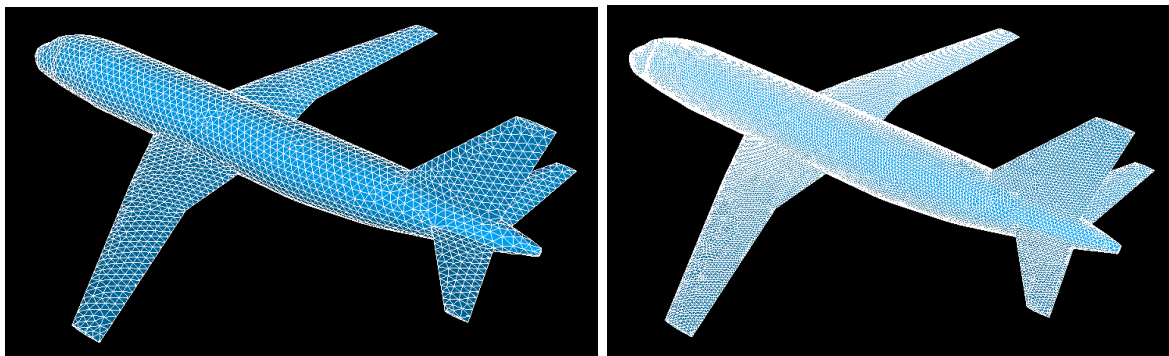


Figure 3: Airbus A319: Mesh 1 and Mesh 2.

To derive the approximation (21) for A_μ , we carry out EIM^g to approximate

$$g(\mu, r) := \exp(i\mu r), \quad r = |x - y|, \quad x, y \in \Gamma. \quad (30)$$

We choose $\mu \in \mathcal{P}_{\text{trial}} := \{0.005, 0.01, \dots, 2.5\}$, a set of 1000 values for the wave number, so that the highest wave number for the source corresponds to a wavelength 5 times larger than the

mean edge of Mesh 1. A natural choice for the discrete set of values for x and y is the set of Gauss points associated with the considered mesh, on which the quadrature formulae used to compute the integrals (29) are defined. The associated discrete set of values for $r = |x - y|$ is roughly proportional to the square of the number of Gauss points, and equals 7.8×10^6 for Mesh 1. To reduce the computational cost, a subsample of 10^5 values for r , that has a very close density to the one obtained from the set of Gauss points, is chosen, see Figure 4.

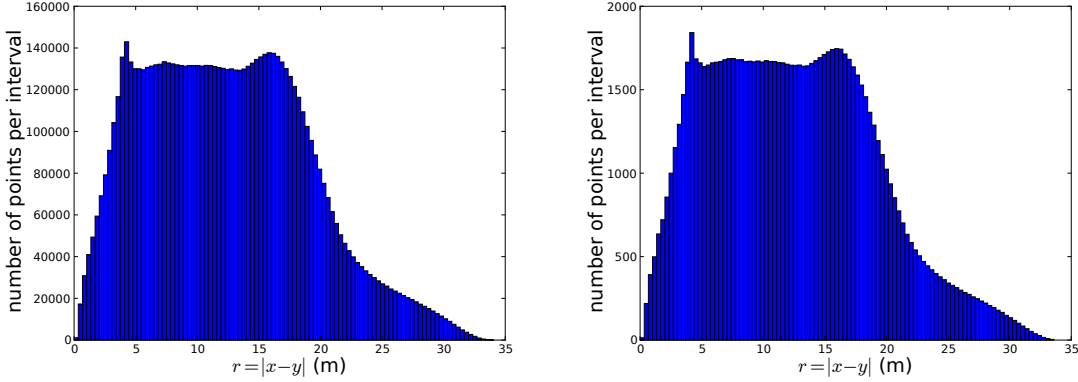


Figure 4: Histograms: discrete values of $r = |x - y|$ over the Gauss points from Mesh 1 (left), and chosen set of size 10^5 (right).

Once EIM^g has been carried out, we can write

$$A_\mu \approx (1 + \mu^2) \sum_{m=1}^{d^g} \lambda_m^g(\mu) M_m,$$

where the matrices M_m have been defined in Section 4.1, so that the approximation (21) can be written using

$$z_p(\mu) := \begin{cases} \lambda_m^g(\mu), & 1 \leq m \leq d^g, \quad p = m, \\ \mu^2 \lambda_m^g(\mu), & 1 \leq m \leq d^g, \quad p = m + d^g. \end{cases} \quad (31)$$

Note that we exploited the links in the functional dependence on μ for the two terms on the right-hand side of (29) to carry out only one EIM^g procedure.

EIM^g and EIM^z are carried out with respectively $d^g = 30$ and $d^z = 32$ interpolation points (notice that $d_{\max} = 60$). To check the accuracy of the approximation, we compute the relative Frobenius norm error on the matrix A_μ and the relative Euclidian norm error on the acoustic pressure computed using the approximate matrix, on a network of 400 points located behind the aircraft. Figure 5 presents the results on Mesh 1. In this figure, the relative differences are computed on 100 values of μ , namely one tenth of the considered parameter values, explaining why only 7 minima are achieved on the left plot. On the right plot concerning the acoustic pressure behind the aircraft, a large number of values are at the level of machine precision. Note that the right-hand side of (28) also depends on the parameter μ . To compute the right plot of Figure 5, we computed the exact values of this right-hand.

Figure 6 shows the solution to the problem on Mesh 1 and the relative difference of the solution using the exact matrix and its approximation for $\mu = 2.47$.

The simulation is repeated on Mesh 2, with $d^g = 50$ and $d^z = 50$. A twice as large frequency interval is considered since Mesh 2 has a better spatial resolution than Mesh 1.

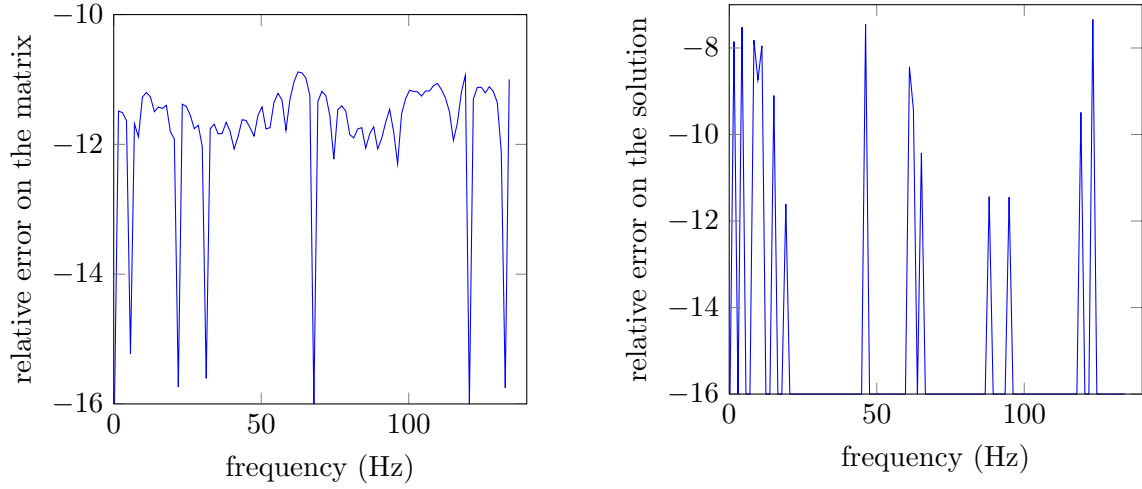


Figure 5: Mesh 1, \log_{10} of the relative error on the Frobenius norm of the matrix A_μ (left), and on the acoustic pressure computed using the approximate matrix on a network of 400 points located behind the plane in Euclidian norm (right), with $d^g = 30$ and $d^z = 32$.

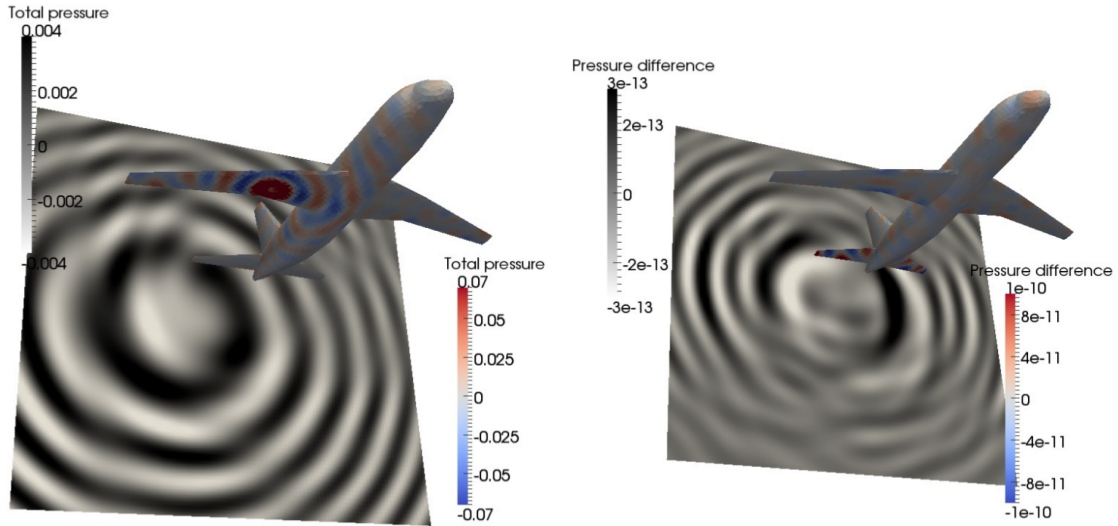


Figure 6: Mesh 1: total acoustic field on the plane and on the network of points (left), and difference between the exact and approximate solution (right), for $\mu = 2.47$.

Figure 7 shows the relative Frobenius norm error on the matrix A_μ , confirming the accuracy of the approximation.

5.3 Sound-hard scattering in a non-uniform flow

Consider an ellipsoid with major axis directed along the z -axis. This object is included inside a larger ball, see Figure 8. The external border of the ball after discretization is denoted by Γ_∞ . The complement of the ellipsoid in the ball is denoted by Ω^- . A potential flow is precomputed around the ellipsoid and inside the ball, such that the flow is uniform outside the ball, of Mach number 0.3 and directed along the z -axis. The flow is fixed, and does not

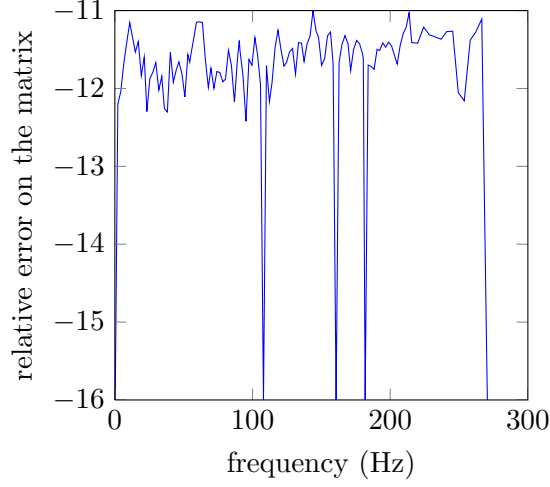


Figure 7: Mesh 2, \log_{10} of the relative error on the Frobenius norm of the matrix A_μ , with $d^g = 50$ and $d^z = 50$.

depend on the parameter μ . An acoustic monopole source lies upstream of the ball, on the z -axis as well. The parameter is again the wave number of the monopole source.

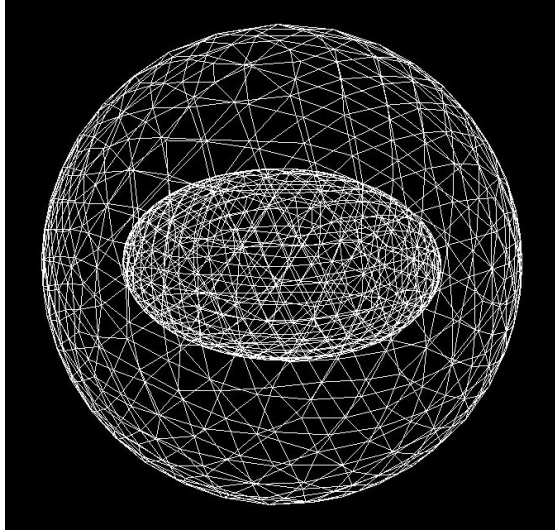


Figure 8: Representation of the mesh.

The considered formulation is a coupled Finite Element Method (FEM) - BEM formulation described in [3]. It consists in (i) applying a change of variable to transform the convected Helmholtz equation into the classical Helmholtz equation outside the ball, in order to apply a standard BEM, and (ii) stabilizing the formulation to avoid resonant frequencies associated with the eigenvalues of the Laplacian inside the ball of border Γ_∞ . The formulation depends on the wave number of the source in a complex way, but we will see in our numerical tests that our nonintrusive procedure provides an accurate approximation of the resulting matrix as a linear combination of a few snapshots of the complete matrix at some wave numbers of the source.

Consider the product space $\mathbb{H} := H^1(\Omega^-) \times H^{-\frac{1}{2}}(\Gamma_\infty) \times H^1(\Gamma_\infty)$ with inner product $((\Phi, \lambda, p), (\Phi^t, \lambda^t, p^t))_{\mathbb{H}} := (\Phi, \Phi^t)_{H^1(\Omega^-)} + (\lambda, \lambda^t)_{H^{-\frac{1}{2}}(\Gamma_\infty)} + (p, p^t)_{H^1(\Gamma_\infty)}$. The weak formulation is: Find $(\Phi, \lambda, p) \in \mathbb{H}$ such that $\forall (\Phi^t, \lambda^t, p^t) \in \mathbb{H}$,

$$\mathcal{V}_\mu(\Phi, \Phi^t) + (N_\mu(\gamma_0^- \Phi), \gamma_0^- \Phi^t)_{\Gamma_\infty} + \left(\left(\tilde{D}_\mu - \frac{1}{2}I \right) (\lambda), \gamma_0^- \Phi^t \right)_{\Gamma_\infty} = (\gamma_1 f_{\text{inc}\mu}, \gamma_0^- \Phi^t)_{\Gamma_\infty}, \quad (32a)$$

$$\left(\lambda^t, \left(D_\mu - \frac{1}{2}I \right) (\gamma_0^- \Phi) \right)_{\Gamma_\infty} - (\lambda^t, S_\mu(\lambda))_{\Gamma_\infty} - i(\lambda^t, p)_{\Gamma_\infty} = -(\lambda^t, \gamma_0 f_{\text{inc}\mu})_{\Gamma_\infty}, \quad (32b)$$

$$(N_\mu(\gamma_0^- \Phi), p^t)_{\Gamma_\infty} + \left(\left(\tilde{D}_\mu + \frac{1}{2}I \right) (\lambda), p^t \right)_{\Gamma_\infty} - \delta_{\Gamma_\infty}(p, p^t) = (\gamma_1 f_{\text{inc}\mu}, p^t)_{\Gamma_\infty}, \quad (32c)$$

where $(\cdot, \cdot)_{\Gamma_\infty}$ denotes the extension of the $L^2(\Gamma_\infty)$ -inner product to the duality pairing on $H^{-\frac{1}{2}}(\Gamma_\infty) \times H^{\frac{1}{2}}(\Gamma_\infty)$, and where

$$\delta_{\Gamma_\infty}(p, q) := \left(\vec{\nabla}_{\Gamma_\infty} p, \vec{\nabla}_{\Gamma_\infty} q \right)_{\Gamma_\infty} + (p, q)_{\Gamma_\infty}, \quad (33)$$

with $\vec{\nabla}_{\Gamma_\infty}$ the surfacic gradient on Γ_∞ , and

$$\mathcal{V}_\mu(\Phi, \Phi^t) := \int_{\Omega^-} \Xi \vec{\nabla} \bar{\Phi} \cdot \vec{\nabla} \Phi^t - \mu^2 \int_{\Omega^-} \beta \bar{\Phi} \Phi^t + i\mu \int_{\Omega^-} \vec{V} \cdot (\bar{\Phi} \vec{\nabla} \Phi^t - \Phi^t \vec{\nabla} \bar{\Phi}), \quad (34)$$

where $\beta := r \left((\varsigma + \gamma_\infty^2 P)^2 - \gamma_\infty^4 M_\infty^2 \right)$, $\vec{V} := r \left((\varsigma + \gamma_\infty^2 P) \mathcal{N} \vec{M} - \gamma_\infty^3 \vec{M}_\infty \right)$, $\Xi := r \mathcal{N} \mathcal{O} \mathcal{N}$ with $r := \frac{\rho}{\rho_\infty}$, $\varsigma := \frac{c_\infty}{c}$, $\gamma_\infty := \frac{1}{\sqrt{1 - M_\infty^2}}$, $P := \vec{M} \cdot \vec{M}_\infty$, $\mathcal{N} := I + C_\infty \vec{M}_\infty \vec{M}_\infty^T$, $\mathcal{O} := I - \vec{M} \vec{M}^T$, and $C_\infty := \frac{\gamma_\infty - 1}{M_\infty^2}$. In the above notation, the subscript ∞ is used for quantities outside the ball, ρ is the density of the flow, c is the speed of sound when the flow is at rest and $\vec{M} = \frac{\vec{v}}{c}$, where \vec{v} is the velocity of the flow. The operators γ_0 and γ_1 are Dirichlet and Neumann traces on the coupling surface Γ_∞ . The operators N_μ , D_μ , \tilde{D}_μ , and S_μ are boundary integral operators, expressed in terms of the Green kernel $G_\mu(x, y) = \frac{\exp(i\mu|x-y|)}{4\pi|x-y|}$ associated with the Helmholtz equation at wave number μ .

The next step is to identify the dependencies in μ in the formulation (32). It turns out that the functions of μ involved in the integrals of the formulation (32) are μ , μ^2 , $\exp(i\mu r)$, $\mu \exp(i\mu r)$, $\mu^2 \exp(i\mu r)$, and $\mu \left(\frac{2i\pi\mu}{c} \mu - 1 \right) \exp(i\mu r)$. As in the previous test case, EIM^g is carried out to approximate the function $g(\mu, r) = \exp(i\mu r)$, $r = |x - y|$, $x, y \in \Gamma_\infty$. We choose $\mu \in \mathcal{P}_{\text{trial}} := \{10, 10.03, \dots, 40\}$, a set of 1000 values for the wave number, so that the highest wave number of the source corresponds to a wavelength 5 times larger than the mean edge of the mesh. This time, instead of considering a subset of $|x - y|$ where x and y are the Gauss points associated with the mesh, we take $r \in \{0, h, \dots, Nh\}$, where $N = 10000$ and $h = \frac{D}{N}$, D being the diameter of the sphere Γ_∞ . With this choice, we no longer need to know the position of the Gauss points, but simply the diameter of the geometry of the test case.

Then, the functions $(\lambda_m^g(\mu))_{1 \leq m \leq d_g}$, $\mu \in \mathcal{P}_{\text{trial}}$, are computed using (12), and the functions

$z_p(\mu)$, $1 \leq p \leq d_{\max} := 4d^g + 3$, are defined by

$$z_p(\mu) := \begin{cases} \lambda_m^g(\mu), & 1 \leq p \leq d^g, & m = p, \\ \mu \lambda_m^g(\mu), & d^g + 1 \leq p \leq 2d^g, & m = p - d^g, \\ \mu^2 \lambda_m^g(\mu), & 2d^g + 1 \leq p \leq 3d^g, & m = p - 2d^g, \\ \mu \left(\frac{2i\pi}{c} \mu - 1 \right) \lambda_m^g(\mu), & 3d^g + 1 \leq p \leq 4d^g, & m = p - 3d^g, \\ 1, & p = 4d^g + 1, \\ \mu, & p = 4d^g + 2, \\ \mu^2, & p = 4d^g + 3. \end{cases} \quad (35)$$

EIM^g and EIM^z are carried out with respectively 17 and 20 interpolation points (notice that $d_{\max} = 71$).

Figure 9 shows the relative Frobenius norm error on the matrix A_μ and the relative Euclidian norm error on the acoustic pressure computed using the approximate matrix on a network of 400 points located behind the scattering ellipsoid. In this test case, an excellent accuracy is obtained with only 20 precomputed matrices.

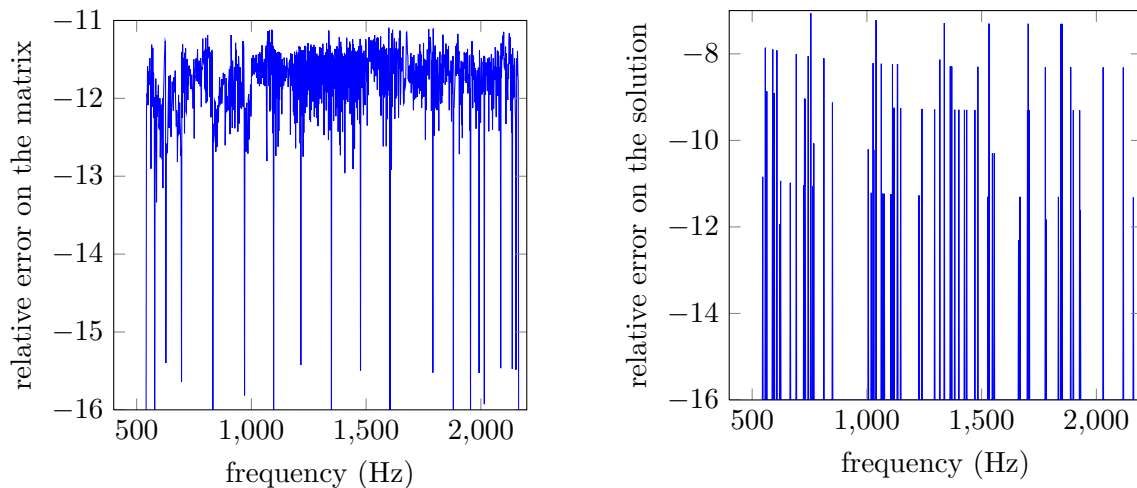


Figure 9: Log₁₀ of the relative error on the Frobenius norm of the matrix A_μ (left) and on the acoustic pressure computed using the approximate matrix computed using (21) on a network of 400 points located behind the object in Euclidian norm (right), with $d^g = 17$ and $d^z = 20$.

6 Conclusion and outlook

The method described herein provides an efficient nonintrusive approximation of parameter-dependent linear systems, provided that the considered code can return the assembled matrix and that the corresponding weak formulation is known. The method offers a crucial practical advantage over existing methods since it avoids significant implementation efforts. In the present work, the choice has been made to approximate the whole matrix A_μ assembled by the code, but the procedure applies in the same way to the approximation of any linear

functional l of the matrix A_μ , whereby

$$l(A_\mu) \approx \sum_{m=1}^{d^z} \beta_m^z(\mu) l(A_{\mu_m^z}), \quad (36)$$

where the storage of $A_{\mu_m^z}$ for all $1 \leq m \leq d^z$ is replaced by the storage of $l(A_{\mu_m^z})$ for all $1 \leq m \leq d^z$, which may be much lighter in terms of memory usage. The efficient construction of the reduced matrix \hat{A}_μ in the RBM corresponds to $l(A_\mu) = U^t A_\mu U$, as explained in the introduction.

Finally, we observe that in the case where the right-hand side C of the problem (6) is also dependent on the parameter μ (then written C_μ), the same procedure can be applied to derive a separated representation of C_μ .

Acknowledgement

This work was partially supported by EADS Innovation Works.

References

- [1] <http://www-hpc.cea.fr/en/complexe/tgcc-curie.htm>.
- [2] P. Binev, A. Cohen, W. Dahmen, R. A. DeVore, G. Petrova, and P. Wojtaszczyk. Convergence rates for greedy algorithms in reduced basis methods. *SIAM J. Math. Analysis*, pages 1457–1472, 2011.
- [3] F. Casenave, A. Ern, and G. Sylvand. A coupled boundary element/finite element method for the convected Helmholtz equation with non-uniform flow in a bounded domain. *arXiv preprint arXiv:1303.6923*, 2013.
- [4] A. Delnevo and I. Terrasse. Code ACTI3S harmonique, justification mathématique, Partie I. Technical report, EADS, 2001.
- [5] A. Delnevo and I. Terrasse. Code ACTI3S, justifications mathématiques, Partie II : présence d’un écoulement uniforme. Technical report, EADS, 2002.
- [6] Y. Maday, N.C. Nguyen, A.T. Patera, and S. Pau. A general multipurpose interpolation procedure: the magic points. *Communications On Pure And Applied Analysis*, 8(1):383–404, 2008.
- [7] J.C. Nédélec. *Acoustic and Electromagnetic Equations: Integral Representations for Harmonic Problems*. Number vol. 144 in Applied Mathematical Sciences. Springer, 2001.
- [8] C. Prud’homme, D.V. Rovas, K. Veroy, L. Machiels, Y. Maday, A.T. Patera, and G. Turinici. Reliable real-time solution of parametrized partial differential equations: Reduced-basis output bound methods. *CJ Fluids Engineering*, 124:70–80, 2002.
- [9] M.L. Stein. *Interpolation of spatial data: some theory for kriging*. Springer Series in Statistics Series. Springer London, Limited, 1999.